Structural rearrangements during mesomorphic phase transitions in poly{10-[(cyano-4′-biphenyl)oxy]decanyl vinyl ether}

V. Tsukruk and J. H. Wendorff
Deutsches Kuntststoff Institut, 6100 Darmstadt, Germany

and Virgil Percec* and Myongsoo Lee
Department of Macromolecular Science, Case Western Reserve University, Cleveland, OH 44106, USA
(Received 31 December 1991; revised 15 April 1992)

The structures displayed by poly{10-[(4-cyano-4′-biphenyl)oxy]decanyl vinyl ether} were studied by small- and wide-angle X-ray scattering. It is shown that this polymer possesses two different smectic phases: an ordered smectic E phase at low temperatures, and a smectic A phase at higher temperatures. The smectic A phase is characterized by a double-layer packing with partial overlap of the cyanobiphenyl groups, while the ordered smectic E phase displays a layer packing characterized by the presence of two incommensurate periodicities. The structural rearrangements accompanying the phase transformation from the ordered to the disordered smectic phase are discussed in detail.

(Keywords: liquid-crystalline polymers; poly(vinyl ether); structure; ordered smectic phases; phase transformations; X-ray scattering)

INTRODUCTION

In recent years, interest in poly(vinyl ether)s containing mesogenic side-groups has increased mainly because they can be synthesized by a living polymerization reaction[1–8]. Our investigations on the polymerization of mesogenic vinyl ethers were performed with the initiating system $CF_3SO_3H/(CH_3)_2S$, which leads to a living polymerization at 0°C in methylene chloride[9,10]. So far, we have elucidated the influence of molecular weight on the phase transitions of poly{ω-[(4-cyano-4′-biphenyl)oxy]-alkyl vinyl ether}s with flexible spacers containing 2–11 methylenic units[11–16], and of some other mesogenic vinyl ethers[17–19]. These results have demonstrated that the nature and the number of mesophases exhibited by side-chain liquid-crystalline polymers are most of the time molecular-weight-dependent. In addition, living copolymerization experiments were used to tailor-make copolymers exhibiting nematic, smectic A and re-entrant nematic phases[11–24].

Poly{10-[(4-cyano-4′-biphenyl)oxy]decanyl vinyl ether} (poly(**6–10**)) with degrees of polymerization higher than 16 exhibits an unidentified smectic mesophase followed by an enantiotropic smectic A mesophase[11–16]. In order to provide a complete elucidation of the phase behaviour of poly(**6–10**), we must understand the structural arrangement of the polymer side-groups in its different liquid-crystalline states.

The goal of this paper is to elucidate the phase behaviour and the structural rearrangements of the layer and intralayer ordering during the phase transitions between the liquid-crystalline states of poly(**6–10**) with a degree of polymerization of 19.

EXPERIMENTAL

Materials

The synthesis of 10-[(4-cyano-4′-biphenyl)oxy]decanyl vinyl ether (**6–10**), its living cationic polymerization initiated with $CF_3SO_3H/S(CH_3)_2$ in CH_2Cl_2 at 0°C, and the characterization of the resultant polymers were presented in previous publications from our laboratory[11–16]. *Table 1* summarizes the polymerization

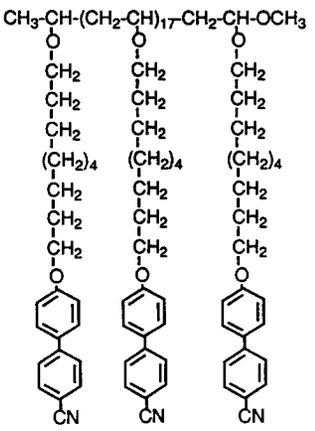

Scheme 1 The structure of poly{10-[(4-cyano-4′-biphenyl)oxy]-decanyl vinyl ether} (poly(**6–10**))

*To whom correspondence should be addressed

0032-3861/93/030481-06

Table 1 Cationic polymerization of **6–10** and characterization of the resulting polymer

$[M]_0/[I]_0$	$M_n \times 10^{-3}$	M_w/M_n (g.p.c.)	*DP*	Phase transitions (°C) and corresponding enthalpy changes (kcal/mru)	
				Heating	Cooling
20	7.3	1.14	19.0	g 15.5 k 55.0 (2.39) s_A 153.7 (0.76) i g 16.2 s_X 44.9 (0.68) s_A 152.9 (0.74) i	i 147.3 (0.72) s_A 37.4 (0.80) s_X 11.8 g

results. The structure of this polymer is shown in *Scheme 1*.

Techniques

Differential scanning calorimetry measurements were performed on a Perkin–Elmer DSC-4 instrument equipped with a TADS data station (model 3600). Heating and cooling rates were 20°C min^{-1}. First-order transitions were recorded at the maximum of the endothermic or exothermic peaks. A Carl–Zeiss optical polarized microscope (magnification 100×) equipped with a Mettler FP 82 hot stage and a Mettler FP 800 central processor was used to observe the thermal transitions and to analyse the anisotropic textures. Before the X-ray experiments, the polymer sample was heated to isotropic temperature, cooled very slowly to the liquid-crystalline state during 10 h and then annealed at 35°C for 1 day. Oriented samples were obtained by very slow step-by-step cooling from the isotropic state to 35°C during 1 week in a magnetic field of 1 T. Wide-angle X-ray scattering (WAXS) curves were recorded on a Siemens D-400 diffractometer. Small-angle X-ray scattering (SAXS) curves were obtained on a compact Kratky camera with positional detector. X-ray photo-patterns on oriented samples were obtained on flat cameras with different sample–film distances. In all cases Ni-filtered Cu Kα radiation was used. Before the measurements the sample was kept at the desired temperature for at least 1 h. The accuracy of the temperature of the thermostated sample was about ±1°C. The analysis of the SAXS data was made by using the programs FFSAXS. This program includes the smoothing of the data by cubic polynomials, subtraction of the background and calculation of the one-dimensional correlation function $G(x)$ by cosine–Fourier transformation of the Lorentz-corrected data. The analysis of the WAXS data was performed by using the program FIT, which includes the smoothing of the data by splines, subtraction of the diffuse background and fitting of the observed maxima by various scattering functions. Additional experimental details on the characterization by WAXS and SAXS and on the processing of the results were presented elsewhere[25].

The spatial arrangement and the geometric sizes of the molecular fragments were analysed for two conjugated monomeric units by the modelling program INSIGHT and the most favourable conformation was calculated by using the program DISCOVER (both from Biosym, San Diego, CA, USA) on a Silicon Graphics workstation.

RESULTS AND DISCUSSION

A poly(**6–10**) with degree of polymerization equal to 19 and $M_w/M_n = 1.14$ was used in all investigations. The

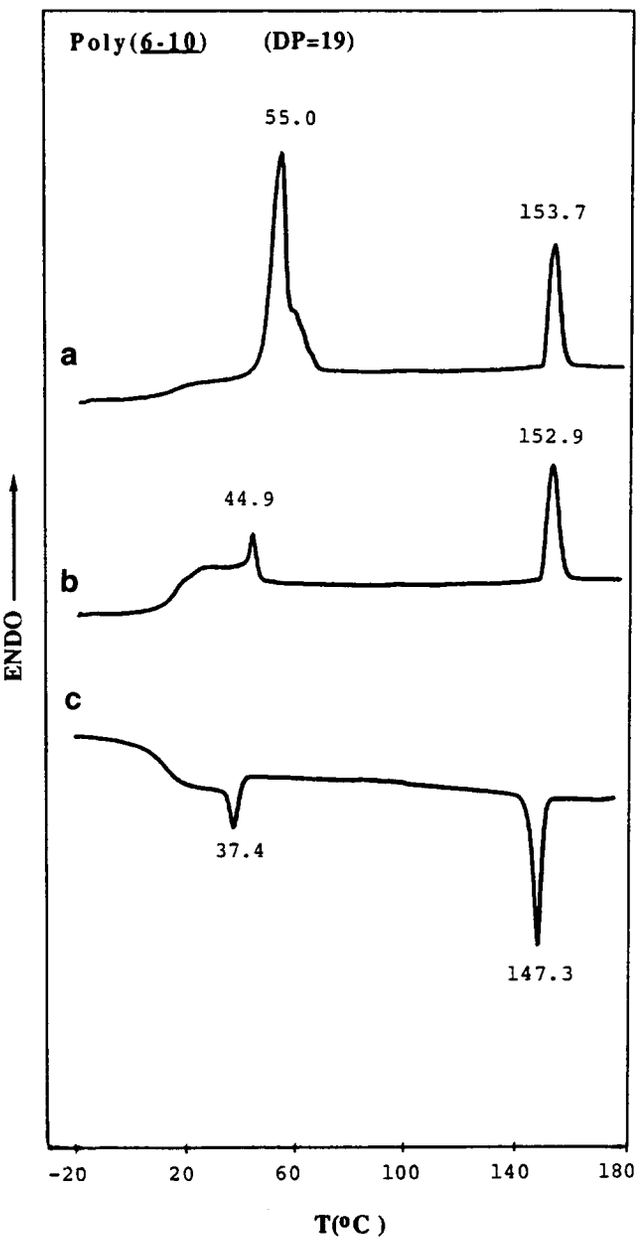

Figure 1 Heating and cooling d.s.c. traces (20°C min^{-1}) of poly(**6–10**) with $DP = 19$: (a) first heating scan; (b) second and subsequent heating scans; (c) first and subsequent cooling scans

d.s.c. thermograms of this polymer are shown in *Figure 1*. In both the heating and the cooling scans, the low-temperature unidentified smectic phase is separated from the high-temperature smectic A phase by a first-order transition (*Figure 1*). Under the optical polarized microscope, the high-temperature mesophase exhibits a focal conic texture, which is characteristic of

a smectic A phase, while the low-temperature phase shows a broken focal conic texture. Both textures were published in previous papers from our laboratory[11–16]. To elucidate the possible structure and the nature of the mesomorphic transition between these two phases, the structure of the low-temperature phase and the parameters of structural packing in the smectic A phase are first determined. Later we will discuss the corresponding structural rearrangements during this phase transition.

Low-temperature smectic phase

On the WAXS curves obtained at low temperatures, two different sets of scattering peaks were observed: two very strong sharp peaks at 2.6° and 5.2° overlapped with a diffuse halo at 6–7° and a modulated broad peak consisting of some overlapped maxima in the range of 20° (*Figure 2*). On the corresponding SAXS curves, these two sharp peaks can be seen more clearly and an additional diffuse halo around 1° is also detected (*Figure 3*). The *d*-spacings of these X-ray data were calculated according to the Bragg law and are presented in *Table 2*.

In the X-ray patterns of the polymer oriented in a magnetic field, one can observe a meridional arrangement of the SAXS reflections, while all three sharp WAXS reflections are concentrated in very widely spread equatorial arcs (*Figures 2* and *3*).

The presence on the WAXS curves of three overlapped peaks points to the formation of ordered intralayer packing of the mesogenic groups in the low-temperature smectic phase. The WAXS maximum was split into three sharp maxima of Lorentz shape with half-widths of about 2° (*Table 2* and *Figure 4*). The absolute value of the intralayer correlation length $\xi_\perp$ is in the range of 1.4 nm. This value is much higher than values typical for disordered smectic phases (0.3–0.6 nm) but slightly lower than typical ones observed for an ordered smectic phase in side-chain liquid-crystalline polymers[25–28]. The correlations in the intralayer ordering ($L \approx 3$ to $4\,\xi$) are extended to 5–6 nm. Thus the regions with ordered intralayer packing include more than 100 mesogenic groups, which corresponds to the existence of a two-dimensional lattice. As judged from the X-ray patterns, the mesogenic side-groups are oriented along the direction of the magnetic field (*Figures 2* and *3*) and

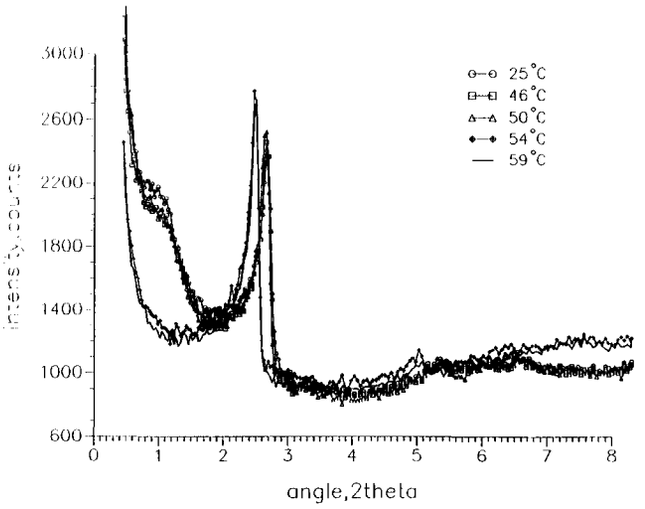

Figure 3 Small-angle X-ray scattering curves of poly(**6–10**) at different temperatures

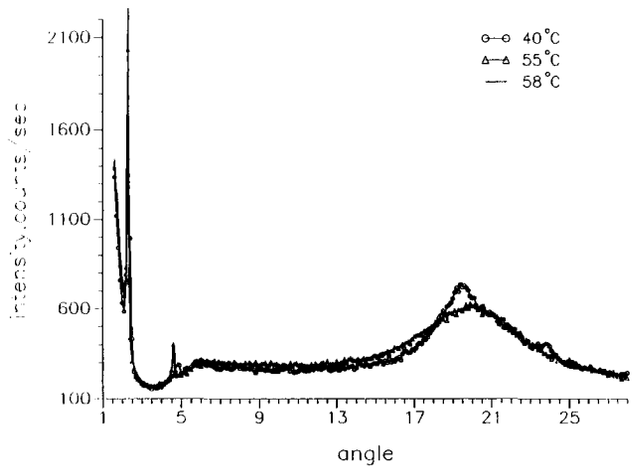

Figure 2 Wide-angle X-ray scattering curves of poly(**6–10**) at different temperatures

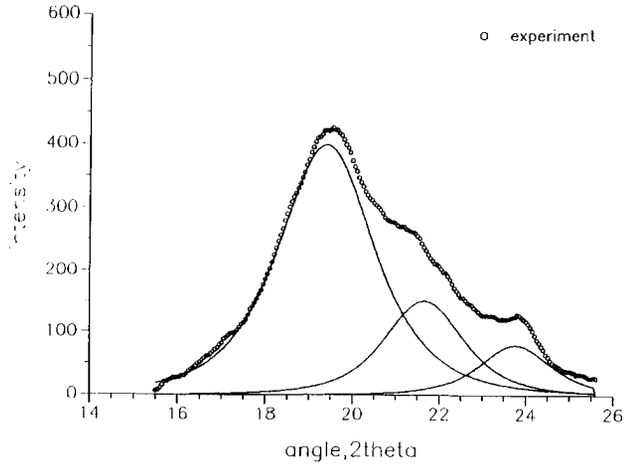

Figure 4 Split of the WAXS for the smectic E phase of poly(**6–10**) by Lorentz profiles

Table 2 Structural characteristic of poly(**6–10**)

	Temperature (°C)	*d*-spacings (nm)[a]							$\xi_\parallel$	$\xi_\perp$
		1	2	3	4	5	6	7		
LC I state	25, cooled		3.17	1.59					45	
	25, annealed 2 h	8.8 w	3.33	1.63	1.3 w	0.454				0.5
	25, annealed 1 day	8.8 w	3.36	1.65	1.3 w	0.457	0.41	0.374	35	1.4
LC II state	59		3.52	1.76	1.1 w	0.45			>100	0.4

[a]The accuracy of *d*-spacings in SAXS region is 0.5 nm for sharp peaks and 0.1 nm for weak ones; in WAXS region the accuracy is 0.005 nm; w = weak intensity

are arranged into layers orthogonally to the smectic plane.

The presence in the WAXS angular region of three sharp peaks orthogonally arranged according to the SAXS layered reflections is typical for a smectic E phase with orthorhombic symmetry of the two-dimensional lattice[28,29]. The positions of all reflections are indexed quite well as the 0 2 0, 1 0 0 and 1 1 0 reflections of the orthorhombic unit cell with parameters $a = 0.4$ nm, $b = 0.914$ nm and $c = 3.36$ nm. Such a lattice is formed by herringbone-packed mesogenic groups with two different orientations of their short axes in the layer planes[26–28]. Thus from the analysis of all available data, we can conclude that the low-temperature phase is a smectic E phase with two-dimensional intralayer packing of orthorhombic symmetry[29,30].

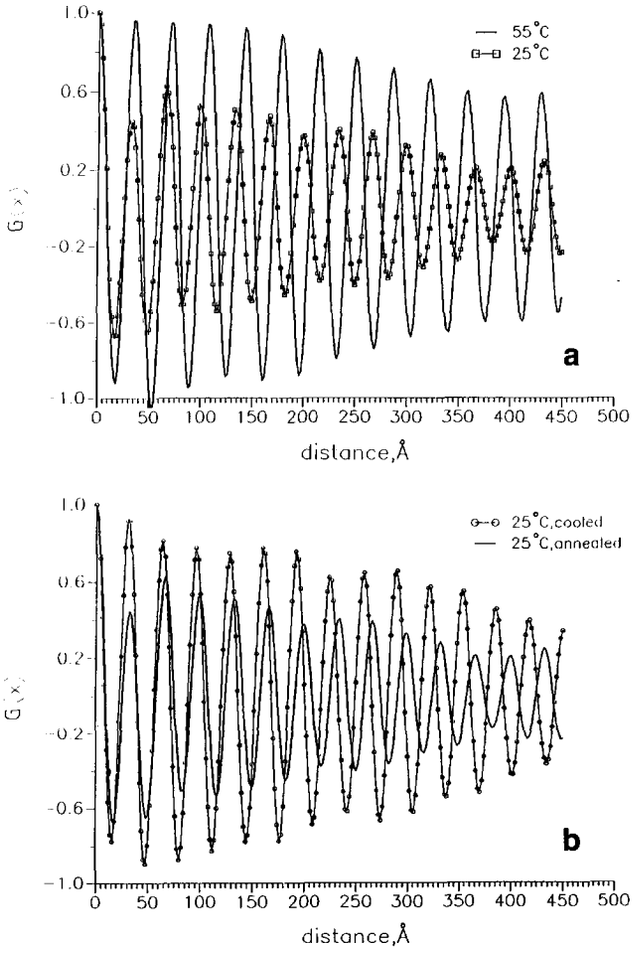

Figure 5 One-dimensional correlation function $G(x)$ of poly(**6–10**) in (a) the smectic E and smectic A phases and (b) smectic E phase after cooling and annealing

Let us consider the perfection of the one-dimensional ordering and possible models of longitudinal packing of the macromolecular fragments in this phase. In order to characterize the perfection of the one-dimensional order, we calculated the one-dimensional correlation function $G(x)$ (*Figure 5*). The function $G(x)$ is common for lamellar phases of damped oscillations with a main period of 6.6 nm. The value of the longitudinal correlation length ξ calculated[25] from $G(x)$ is equal to 35 nm. This value is also typical for smectic ordered phases of side-chain polymers with a high concentration of defects formed by coil-like flexible backbones[25–27].

As deduced from the highest intensity of the second maximum of $G(x)$, the main period of the density distribution, which corresponds to the thickness of the layers, is equal to 6.6 nm. Such a periodicity fits quite well with the common double-layer structures of cyano-containing mesogenic groups with partial overlap of the side fragments (*Figure 6*). As judged from conformational calculations, the cyanobiphenyl mesogenic groups are arranged at a definite angle according to the orthogonal direction of the methylene spacer, as shown in *Figure 4*, and in the framework of the proposed packing they are fully overlapped. The main periodicity of 6.6 nm is determined by the distance between backbones arranged in the same plane (*Figure 6*). This distance is twice as high as the *d*-spacing calculated from the position of the first SAXS peak (*Table 2*). We also observe an additional maximum at 3.3 nm, which points to the existence of an additional half-period density wave. This situation is very similar to that discussed in detail for other ordered side-chain smectic polymers[25–28] and demonstrates the existence of an additional periodicity normal to the smectic planes between densely packed mesogenic groups of neighbouring molecules (*Figure 7*). As is well known for layered structures, the existence of

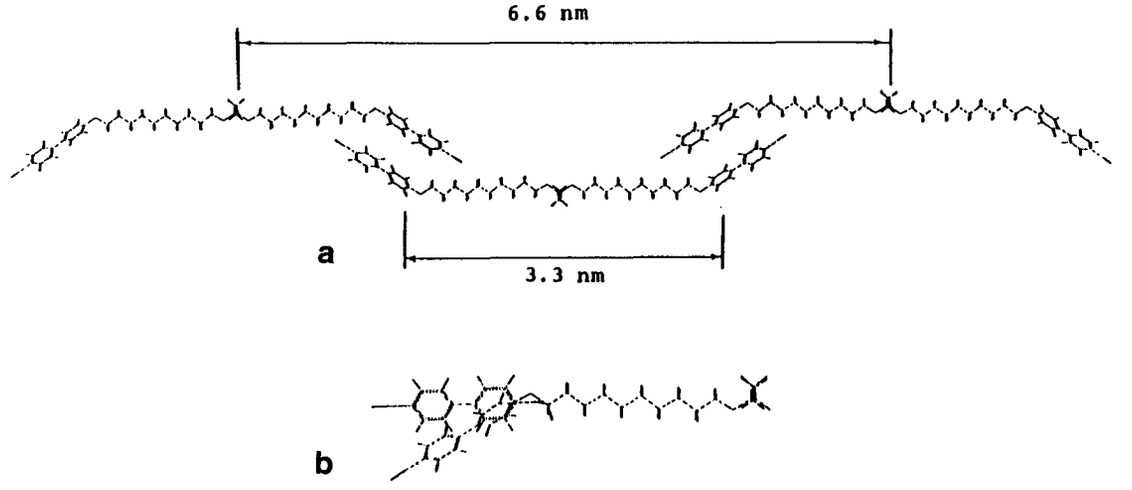

Figure 6 Molecular models of the liquid-crystalline poly(**6–10**): (a) model of double-layer packing with overlapping of the mesogenic groups (main periodicity and half-periodicity are shown); (b) possible changes of the arrangement of the biphenyl mesogenic groups as a result of torsional rotation

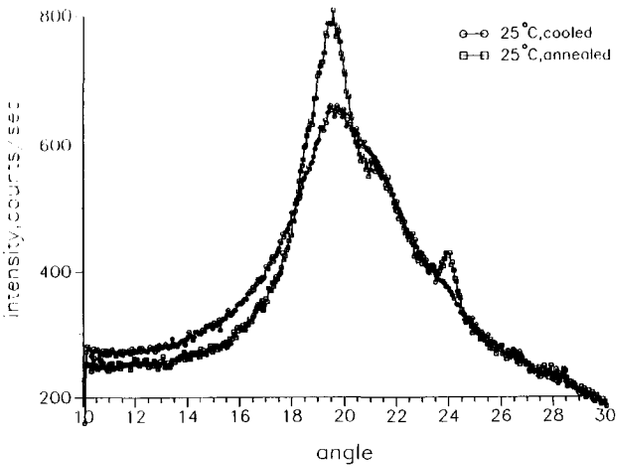

Figure 7 Wide-angle X-ray scattering curves of poly(**6–10**) at 35°C after cooling and annealing during 1 day

such additional half-periods in the density distribution leads to the extinction of odd orders of reflections[29,30]. Thus for the layered packing of the polymer studied, the first-order reflection with $d = 6{,}6$ nm should be extinguished and the observed SAXS peaks are second- and fourth-order reflections of the proposed double-layer packing. Thus from this discussion we can conclude that the low-temperature phase in this polymer is a smectic E phase with orthorhombic intralayer order and double-layer longitudinal packing, and with overlapped cyanobiphenyl mesogenic groups in the side-chains.

High-temperature smectic phase

As was mentioned above, the high-temperature phase in this polymer is most probably the common disordered smectic A phase[29]. From the data obtained, we can conclude that the well defined layered structure is maintained in this phase only with a slightly changed periodicity and liquid-like quasi-hexagonal ordering into layers (*Figures 2* and *3*). As a result of two-dimensional melting of the intralayer lattice, only a short-range order is detected in this phase. The short-range order in the intralayer packing of the mesogenic groups extends only to $L = 1–2$ nm, which is typical for a smectic A mesophase. The thickness of layers of 7 nm is only slightly higher compared to the initial double-layer packing. The perfection of one-dimensional order in the smectic A phase is much higher compared to the ordered smectic E phase. The value of the longitudinal correlation length ξ is resolution-limited and is not lower than 100 nm (*Figure 5*).

Thus the high-temperature phase in this liquid-crystalline polymer is the common disordered smectic A phase with interdigitated double-layer packing, long-range longitudinal ordering and short-range order into layers. It is obvious from comparison of the structural data of these two phases that, during the smectic E–smectic A phase transformation, different changes of the structural ordering are observed such as: melting of the intralayer ordering, change of thickness of the layer packing, and disappearance of the SAXS diffuse halo. All these structural changes will be discussed in the next section.

Structural changes observed during the heating–cooling–annealing cycle

Intralayer packing. Heating of the polymer to T_1 leads only to minor changes of the WAXS scattering, while an increase of temperature to above T_1 causes the appearance of the diffuse halo (*Figure 2*). These changes of WAXS scattering occur in a very narrow temperature interval (2–4°C) near T_1 and correspond to the so-called two-dimensional melting of the intralayer packing during the transition from the ordered to the disordered smectic phase[25–27]. The orthorhombic symmetry of the intralayer packing of the smectic E phase is broken and a common quasi-hexagonal short-range order is formed. The corresponding intralayer correlation length drops abruptly about 3–4 times (from 1.4 to 0.4 nm).

During cooling of the high-temperature phase, the phase transformation occurs at $T_1 = 37$°C (according to the d.s.c. data at a rate of 20°C min^{-1}). But on the WAXS curve this phase transition occurs in 2 h at room temperature. After the sample was slowly cooled at 35°C for 10 h the initial overlapped sharp peaks are restored and the ordered intralayer ordering, which characterizes the smectic E phase, is formed. Consequently, as a result of cooling from the smectic A state into a glassy state, we have generated a metastable structure with liquid-like intralayer order coexisting with the partially transformed ordered phase. This metastable structure could be transformed into the initial ordered smectic E state by prolonged annealing at temperatures higher than the glass transition temperature. This observation is also confirmed by the observed changes of d.s.c. traces for samples with different thermal prehistory.

Layer packing. During the transformation from smectic E to smectic A phase, an increase of the intensity of the SAXS maximum and of the corresponding d-spacings as well as the disappearance of the diffuse halo from around 1° are observed simultaneously (*Figure 3*). All these changes occur very sharply in a narrow interval of 2°C width, i.e. from 54 to 56°C (see for example *Figure 8*). The longitudinal correlations also increase sharply after the transition from the smectic E to the smectic A phase (*Figure 5*). The increase of the thickness of the smectic layers during melting of the intralayer packing can be explained very easily by the free rotation of the mesogenic groups in the smectic A phase. As can be seen from *Figure 5*, the introduction of only one *gauche*

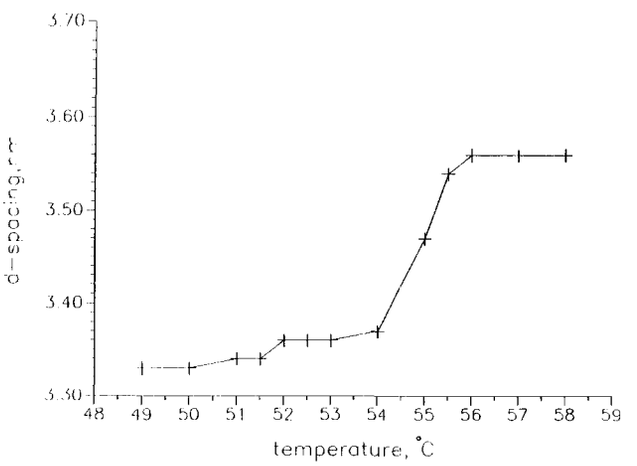

Figure 8 The dependence of d-spacing of poly(**6–10**) on temperature

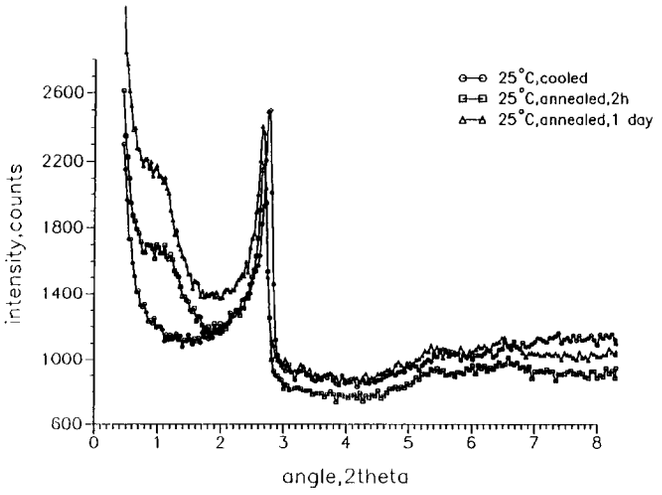

Figure 9 Small-angle X-ray scattering curves of poly(**6–10**) obtained during annealing

conformer into the side-chain leads to the arrangement of the biphenyl moieties along the overall direction of the side-chains. Correspondingly, the projection of one side-chain normal to the smectic plane increases by 0.15–0.2 nm. This leads to an increase of the overall thickness of the initial double-layer packing to 0.3–0.4 nm, which corresponds to the observed value (*Table 2*).

The SAXS curve of the polymer cooled to room temperature from the isotropic state differs from the initial one. The sharp maximum shifts to higher angles and the diffuse one from around 1° is not restored (*Figure 8*). After annealing at 35°C for 2 h the sharp peak is shifted to lower angles and the diffuse maximum at 1° appears. A longer annealing time of about 1 day leads to full restoration of the initial curve of the annealed sample (*Figure 9* and *Table 2*). The longitudinal correlations are lowered very strongly during cooling and the height of the second maximum on $G(x)$ increases (*Figure 5b*). All these data are the result of the quick cooling of the polymer from the isotropic state into the glassy state with a freezing of the smectic A-like structure containing the liquid-like intralayer ordering. The development of the ordered smectic E phase at a temperature higher than T_g is a very slow process, and the formation of the orthorhombic lattice in the intralayer packing of the mesogenic groups with conformational changes in side-groups is accompanied by the appropriate changes of the layer ordering.

CONCLUSIONS

The side-chain liquid-crystalline polymer poly(**6–10**) exhibits two different smectic phases: at low temperature an ordered smectic E phase with orthorhombic intralayer packing of the mesogenic groups, and at high temperature the common disordered smectic A phase. In both phases a double-layer longitudinal packing of the macromolecular fragments with a thickness of 6.6–7 nm and overlapping of the slightly tilted mesogenic groups is realized. In the ordered smectic E phase we detected for the first time the formation of incommensurate coexistent layer packings. During the smectic E to smectic A phase transition, melting of the intralayer packing occurs, which leads also to slight changes of the thickness of the smectic layers as a result of the conformational disordering of the side-chains. The smectic A-like structure could be frozen in the glassy state by quick cooling. The development of the ordered smectic E phase as a result of annealing at temperatures higher than T_g is a very slow process, since it requires the formation of the ordered intralayer orthorhombic packing of mesogenic groups and incommensurate coexistent double-layer packing.

ACKNOWLEDGEMENTS

Financial support from the Office of Naval Research is gratefully acknowledged. V.T. thanks the Humboldt Foundation for financial support.

REFERENCES

1 Rodriguez-Parada, J. M. and Percec, V. *J. Polym. Sci. (A) Polym. Chem.* 1986, **24**, 1363
2 Percec, V. and Tomazos, D. *Polym. Bull.* 1987, **18**, 239
3 Sagane, T. and Lenz, R. W. *Polym. J.* 1988, **20**, 923
4 Sagane, T. and Lenz, R. W. *Polymer* 1989, **30**, 2269
5 Sagane, T. and Lenz, R. W. *Macromolecules* 1989, **22**, 3763
6 Kostromin, S. G., Cuong, N. G., Garina, E. S. and Shibaev, V. P. *Mol. Cryst., Liq. Cryst.* 1990, **193**, 77
7 Heroguez, V., Deffieux, A. and Fontanille, M. *Makromol. Chem., Macromol. Symp.* 1990, **32**, 199
8 Heroguez, V., Schappacher, M., Papon, E. and Deffieux, A. *Polym. Bull.* 1991, **25**, 307
9 Cho, C. G., Feit, B. A. and Webster, W. A. *Macromolecules* 1990, **23**, 1918
10 Lin, C. H. and Matyjaszewsky, K. *Polym. Prepr. Am. Chem. Soc., Div. Polym. Chem.* 1990, **31**(1), 599
11 Percec, V., Lee, M. and Jonsson, H. *J. Polym. Sci. (A) Polym. Chem.* 1991, **29**, 327
12 Percec, V. and Lee, M. *J. Macromol. Sci.–Chem. (A)* 1991, **28**, 651
13 Percec, V. and Lee, M. *Macromolecules* 1991, **24**, 1017
14 Percec, V. and Lee, M. *Macromolecules* 1991, **24**, 2780
15 Percec, V., Lee, M. and Ackerman, C. *Polymer* 1992, **33**, 703
16 Kostromin, S. G., Cuong, N. G., Garina, E. S. and Shibaev, V. P. *Mol. Cryst., Liq. Cryst.* 1990, **193**, 77
17 Percec, V., Gomes, A. and Lee, M. *J. Polym. Sci. (A) Polym. Chem.* 1991, **39**, 1615
18 Percec, V., Wang, C. H. and Lee, M. *Polym. Bull.* 1991, **26**, 15
19 Percec, V., Zheng, Q. and Lee, M. *J. Mater. Chem.* 1991, **1**, 611
20 Percec, V. and Lee, M. *Polym. Bull.* 1991, **25**, 123
21 Percec, V. and Lee, M. *Polym. Bull.* 1991, **25**, 131
22 Percec, V. and Lee, M. *Macromolecules* 1991, **24**, 4963
23 Percec, V. and Lee, M. *Polymer* 1991, **32**, 2862
24 Percec, V. and Lee, M. *J. Mater Chem.* 1991, **1**, 1007
25 Tsukruk, V., Shilov, V. and Lipatov. Y. *Macromolecules* 1986, **19**, 1308
26 Tsukruk, V., Shilov, V. and Lipatov. Y. *Acta Polym.* 1985, **36**, 403
27 Lipatov, Y., Tsukruk, V. and Shilov, V. *J. Macromol. Sci.–Macromol. Chem. Phys. (C)* 1984, **24**, 173
28 Noel, C. in 'Side Chain Liquid Crystal Polymers' (Ed. C. B. McArdle), Chapman and Hall, New York, 1989, p. 159
29 Hefrich, W. *J. Phys. (Paris) Coll.* 1979, **40**, C3
30 Gray, G. W. and Goodby, G. W. 'Smectic Liquid Crystals', Leonard Hill, Glasgow, 1984